ACADEMIA ROMÂNĂ
Revue Roumaine de Chimie
https://www.icf.ro/rrch/

Rev. Roum. Chim.,
2023, *68*(3–4), 173–183
DOI: 10.33224/rrch.2023.68.3-4.07

Dedicated to Dr. Maria Zaharescu
on the occasion of her 85th anniversary

INFLUENCE OF ULTRASONIC TREATMENT AND HEATING/COOLING UNDER ELECTRIC FIELD ON HIGH-*K* CELLULOSE-BARIUM TITANATE COMPOSITES

Răzvan ROTARU, Carmen-Mihaela POPESCU, Andrei DASCĂLU, Daniel ȚÎMPU, Mihai ASĂNDULESA, Maria Emiliana FORTUNĂ and Valeria HARABAGIU*

"Petru Poni" Institute of Macromolecular Chemistry, 41A Grigore Ghica Voda Alley, Iaşi, 700487, Roumania

Received February 4, 2023

The present research reports the ultrasonic assisted synthesis of ferroelectric cellulose-barium titanate composites (C/BT). As proved by wide angle X-ray diffraction (WAXD) and by scanning electronic microscopy (SEM), the composites consist of perovskite-type barium titanate particles (BT) of 400–600 nm, disposed around the cellulose microfibers. Fourier transform infrared spectroscopy (FTIR), (SEM) and (WAXD) investigation revealed the modifications of structure/ morphologies of the prepared sample as compared to pristine cellulose, with direct consequences on the polymer crystalline domains, on the uniformity of BT dispersion and on the dielectric properties of the composites. The composites obtained by ultrasonic treatment possess high dielectric constants (58.6–140.5), better breakdown strengths (8.9–17.7 kV/mm) and energy storage densities (2.6–9.0 J/cm^3) as compared to BT particles, as well as very low dielectric losses (0.27–3 × 10^{-4}) at industrial frequencies (50–55 Hz), the values being dependent on the content of barium titanate and on the preparation parameters.

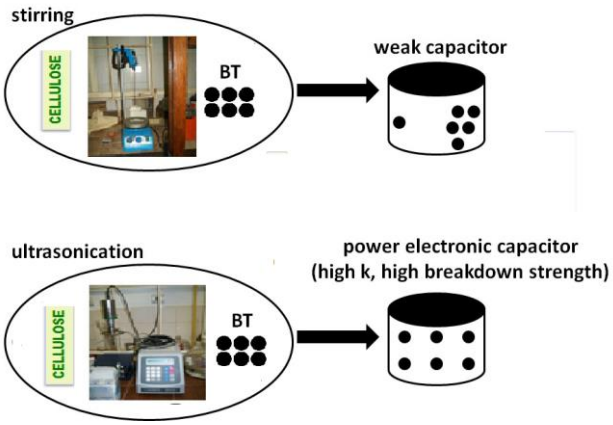

INTRODUCTION

Polymers and polymer-based composites with high dielectric permittivity (dielectric constant), low dielectric loss factor, high breakdown voltage are attractive materials for electronics and electrical industry. Due to their specific properties, such as relatively low processing temperatures and low density as compared to full inorganic equivalents, they offer lots of freedom degrees in the design of new products. The easy variation of their physical properties, such as electric conductivity or dielectric constant, photo-emission, electrostriction strain, electrocaloric effect, gives access to high added values materials.[1-5] For some years the insertion of discrete passive electronic components (capacitors, resistors, and inductors) into the core of a printed circuit board is under intense investigation. For integration of a capacitor into the inner layers of a printed circuit, polymeric materials with high dielectric breakdown, high permittivity and low dielectric loss are needed.

* Corresponding author: hvaleria@icmpp.ro

To get composites of high dielectric constant, appropriate for uses in capacitors, at least one of the precursors should be characterized by a high electronic polarization. Quite often nano- or micro-sized perovskite-type materials (*e.g*. ferroelectric barium titanate), have been considered as high-k (high dielectric constant) fillers. Low dielectric loss involves a good dispersion of the ferroelectric particles into the polymer matrix and a homogeneous packing, in order to minimize the effects of the interfacial polarization common to multi-phase mixtures. This kind of polarization strongly increases the dielectric loss.[6,7] Routinely, grinding, high pressure homogenization or stirring processes were used for mixing the components and high-*k* polymer–ferroelectric composites with a relative permittivity higher than 10 were reported.[3,4]

Based on the well-known effects (acoustic cavitation, thermal, micro-jet and shockwave phenomena), sonication with high-frequency ultrasound (higher than 10 kHz) can offer a good dispersion of the precursors in order to get a homogeneous composite. These extreme conditions can also accelerate some chemical reactions. We previously exploited sonication process to prepare viscose fiber-barium titanate composites for electromagnetic shielding[3] or magnetic cellulose-iron oxide composites.[8] Poly(vinyl alcohol)/cellulose[9,10] and electro-conductive polyaniline/cellulose composites[11] were also prepared by using ultrasounds.

Heat treatment under intense electric field was also proved to increase the electronic polarization and to provide composites with high dielectric constant. The combined effects of this treatment consist in raising the dipole orientation along the external electric field and the injection of charges into the sample due to their increased mobility. Moreover, the application of an external electric field could change the disordered dipolar state into an ordered one due to the reduction of the entropy of the dipolar subsystem in case of the ferroelectric materials (perovskite, poly(vinylidene fluoride), hafnium oxide) with the same consequence of increasing the dielectric constant.[12] The thermally stimulated discharge technique has been already applied by Rotaru *et al.*[3] for viscose-barium titanate composite (heating at 50 °C under 30 kV continuous electric field) and Kubon *et al.*[13] for poly(methyl methacrylate)-based composites (heating to well above the glass transition temperature of the polymer and subjecting the material to an electric field of 20 kV/cm).

Another important aspect of a good capacitor, particular in power electronics when high voltages are required, is related to the dielectric breakdown (or dielectric strength). When high electric fields are applied across the dielectric materials used as capacitors, a large number of electrons may suddenly be excited to energies within the conduction band. As a result, the current through the dielectric increases dramatically, producing localized burning, irreversible degradation and perhaps the failure of the material, which can become an electrical conductor. The maximum electric field to which an insulating material can resist is called breakdown voltage, dielectric breakdown or dielectric strength. Usually, barium titanate has a low breakdown voltage up to 100–180 kV/cm[14], while higher values are registered for polymers, depending on their chemical nature and/or their morphology (*e.g*., 550–650 kV/cm for silicone elastomers substituted with nitrobenzene groups[15] or 255–282 kV/cm for polyimides containing bipyridine units[16]).

The purpose of this work is to provide an efficient method for the preparation of high-k ferroelectric homogeneous cellulose/barium titanate composites. Different preparation conditions were applied (stirring or varied sonication duration and amplitude, additional thermal treatment in the presence of an intense direct electric field) and the structure, morphology and properties (dielectric constant, dielectric loss and dielectric breakdown) of the thus obtained composites were compared with those of the starting materials by means of FTIR, SEM, WAXD, dielectric spectroscopy, and breakdown strength measurements, respectively.

RESULTS AND DISCUSSION

An energy efficient method involving ultrasonic homogenization and microwave assisted drying for the preparation of submicronic barium titanate particles (BT) was previously reported.[17] Owing the known dielectric properties of barium titanate, a sustainable polymer matrix derived from natural resources, namely microcrystalline cellulose was used to obtain polymer/inorganic particle composites. To follow the influence of the preparation conditions on the

structure/morphology/properties of the obtained composites, mechanical stirring and ultrasonic treatment were used for homogenization, while some samples were also heated/cooled under high voltage electric field. The coding and the preparation conditions of significant samples are detailed in the Experimental section and summarized in Table 1.

Table 1

Preparation conditions of cellulose-BT composites

Sample code*	Ultrasonic amplitude [%]**	Stirring or ultrasonication duration [min]	Maximum temperature reached in ultrasonic process [°C]	Thermal treatment in electric field (80 °C, 30 kV)
C/BT_{20st}	-	15	-	No
C/BT_{20a}	50	15	85	No
C/BT_{20b}	50	30	93.9	No
C/BT_{20c}	100	15	94.5	No
C/BT_{40}	50	15	84.5	No
C/BT_{40el}	50	15	84.5	Yes
C_{el}	-	-	-	Yes

*"st" and "el" subscripts denote samples obtained by stirring or thermally treated under electrical field; the number subscripts represent the BT content in the C/BT composite samples (% by weight);
** % from 750 W (nominal power of the ultrasonic device)

Structure/morphology characterization

Infrared spectroscopy (FT-IR) was first used to follow the structure of precursors and of the obtained composites. The method gives information about structural modifications and interactions taking place in composite materials. Figure 1 compares the FT-IR spectra (a) and their derivatives (b) for the microcrystalline cellulose samples and the cellulose/barium titanate composites (C/BT) obtained through different processing conditions. Details on the second derivatives of O-H large bands between 3600 and 3180 cm^{-1} are presented in Fig. 2. The assignments of FT-IR bands and of their maxima observed in the second derivative spectra were made according to the available references for barium titanate[18,19] and for cellulose[22-30](Table 2).

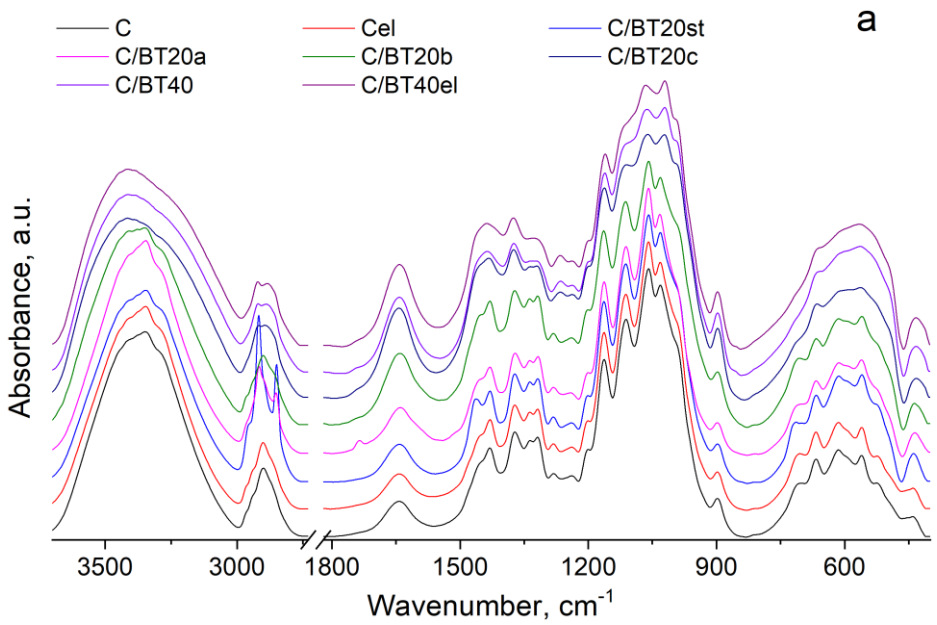

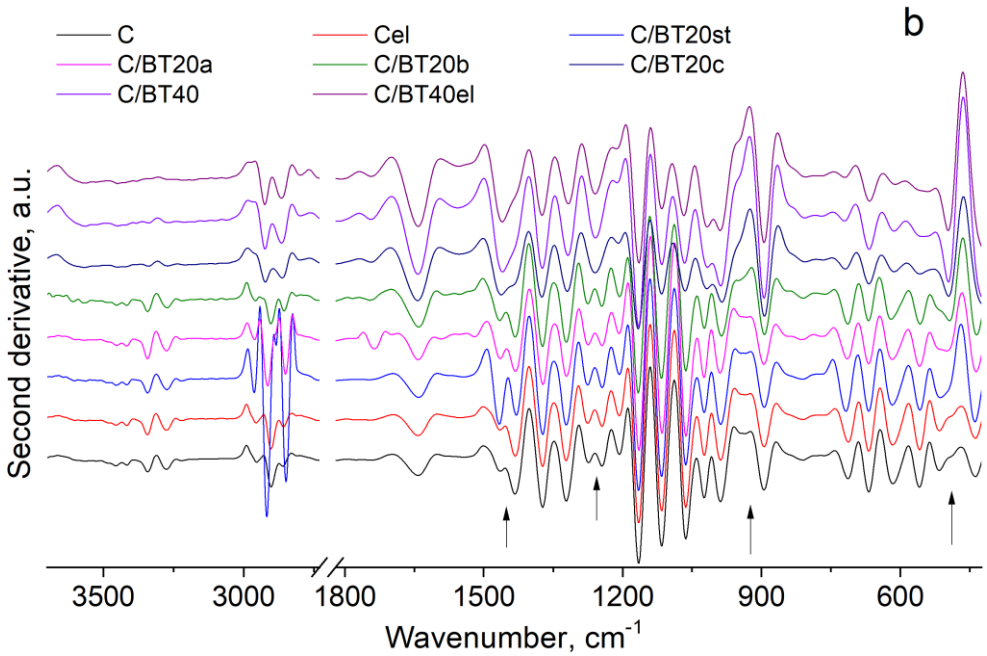

Fig. 1 - Infrared spectra (a) and their second derivatives (b) of the studied samples.

Table 2

The characteristic FT-IR bands their assignments for pure celluloses, barium titanate and C/BT composites

Wavenumber range [cm^{-1}]	Assignment
3564-3211	O-H vibrations
2969-2848	C-H, CH_2 symmetric and asymmetric stretching vibrations
1642-1639	O-H absorbed water
1465-1429	C-H deformations, OH in plane bending vibrations
1374-1314	C-H deformation vibrations, CH_2 rocking vibrations
1148-1020	C-O, C-C stretching vibrations
989-938	C-O pyranose ring stretching
895-842	C-H deformations
750-450	Cellulose bands superposed on BT bands (559 cm^{-1}: Ti-O_I stretching vibration for tetragonal phase; 438 cm^{-1}: Ba-O and Ti-O vibrations)

As one may see from Fig. 1 and Table 2, for all studied samples, the main vibration bands are located in different frequency regions, specific to cellulose, while the bands of barium titanate (559 and 438 cm^{-1}) are covered by those of cellulose in 750-400 cm^{-1} region.

The microcrystalline cellulose spectrum is a typical one for cellulose (Fig. 1a). In 3750 – 2750 cm^{-1} interval, strong absorptions corresponding to different O-H stretching vibrations and prominent methyl and methylene C-H vibrations were identified. The O-H stretching vibration large band is composed of several sub-bands, as seen from the second derivative spectra (Fig. 1b), namely: at 3564 cm^{-1} (stretching vibration of weakly bound adsorbed water), at 3455 and 3416 cm^{-1} (O2–H2-O6 intramolecular hydrogen bonds stretching vibrations), at 3344 cm^{-1} (O5–H5-O3 intramolecular hydrogen bonds stretching vibration), at 3274 and 3223 cm^{-1} (O6–H6-O3 intermolecular hydrogen bonds stretching vibration for the Iβ and Iα cellulose forms). The bands assigned to symmetric and asymmetric stretching vibration of the methyl and methylene groups were identified in the microcrystalline cellulose spectrum at 2953, 2901 cm^{-1} and at 2860, 2810 cm^{-1}, respectively.

Both, the spectrum and second derivative of the electrically treated cellulose (C_{el}) and those of C/BT_{20st} composite do not reveal any difference in this region as compared to the pristine cellulose sample (C), indicating that the thermal treatment

under electric field and the mixing by mechanical stirring with BT particles did not affect the cellulose structure (see details of the second derivative spectra in Fig. 2). Further, the derivatives of all composites prepared by ultrasonic treatment, show modifications of the maxima location and intensity of the intermolecular hydrogen bond band, which depend on both the sonication parameters and the concentration of BT. Therefore, as seen from Fig. 2, for these samples, the shifting of the band from 3223 cm^{-1} in cellulose sample towards lower wavenumbers at 3216–3211 cm^{-1} was observed, meaning higher energies of the intermolecular hydrogen bonding in composite materials as compared to pristine cellulose. The shifting of the maxima may be due to the presence of BT crystals which induce conformational changes in the Iα allomorph structure. Moreover, C/BT_{20b} and C/BT_{20c} samples indicate in the FT-IR second derivative spectrum the appearance of a new band at 3385 cm^{-1} assigned to O-H groups present in the BT structure. When a higher amount of BT was used in the composites (C/BT_{40} and C/BT_{40el}), the band from 3385 cm^{-1} increases in intensity, while the bands assigned to pristine cellulose decrease in intensity. This is an apparent modification due to the presence of a higher amount of BT and lower amount of cellulose in the same quantity of analyzed samples. The shifting of cellulose OH bands towards lower wavenumber induced by interactions with TiO_3^{2-} was also mentioned in literature.[20,21] Moreover, in the spectra of C/BT_{20b}, C/BT_{20c}, C/BT_{40} and C/BT_{40el}, the bands from 3344 and 3274 cm^{-1} decrease in intensity. This indicates a decrease of the number of O5–H5···O3 intramolecular and O6–H6-O3 intermolecular H-bonds from cellulose, which probably participate to formation of bonds with BT.

In 1800–400 cm^{-1} region, all samples indicate specific bands for cellulose as assigned in Table 2, while in 750–400 cm^{-1} interval, the adsorptions of barium titanate particles (559 and 438 cm^{-1}) present in C/BT composite samples are covered by those of cellulose (Fig. 1a). Once again, the spectra of C_{el} and C/BT_{20st} samples did not show any difference in this region, compared to pristine microcrystalline cellulose spectrum and the spectra of C/BT_{20a}, C/BT_{20b} and C/BT_{20c} samples are also quite similar with that of the pristine cellulose. However, when higher concentration of barium titanate was used (namely 40%), noticeable differences were observed in the spectra of the C/BT_{40} and C/BT_{40el} samples as compared to pristine microcrystalline cellulose spectrum. Thus, as better visible in Fig. 1b, the shifting to higher or lower wavenumbers of the CH2 rocking (1321 cm^{-1}), C-H bending (1275 cm^{-1}) and pyranose ring stretching (942 cm^{-1}) bands present in cellulose spectrum to 1316/1314 cm^{-1}, to 1264/1264 cm^{-1}, and to 952/954 cm^{-1}, respectively, as well as the band intensity increase (C-H deformation, O-H in plane bending at 1462 cm^{-1}; C-H bending at cm^{-1} 1264; C-O and C-C stretching ring vibrations at 1020 cm^{-1}) or decrease (C-O-C stretching vibration at 1246/1247 cm^{-1}) could be identified. Moreover, the band located to 435 cm^{-1} in cellulose has also a higher intensity in the spectra of composites, the increase being due to the superposition on the band of BT particles. All these modifications might be due to cellulose structural modifications induced by the presence of inorganic particles through interactions between C and BT by dipole-dipole interactions and hydrogen bonds and/or complexation with the functional groups of the C matrix.

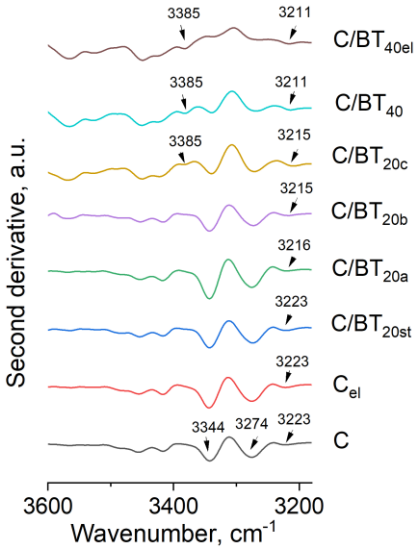

Fig. 2 – Detailed second derivative spectra in the 3600 – 3180 cm^{-1} region revealing the differences between the samples.

Wide angle X-ray diffraction (WAXD) analysis was used to accomplish a deeper structural characterization of the studied materials. The X-ray diffraction patterns for precursors (pristine cellulose, cellulose treated in electric field, barium titanate) and of their composites are depicted in Fig. 3.

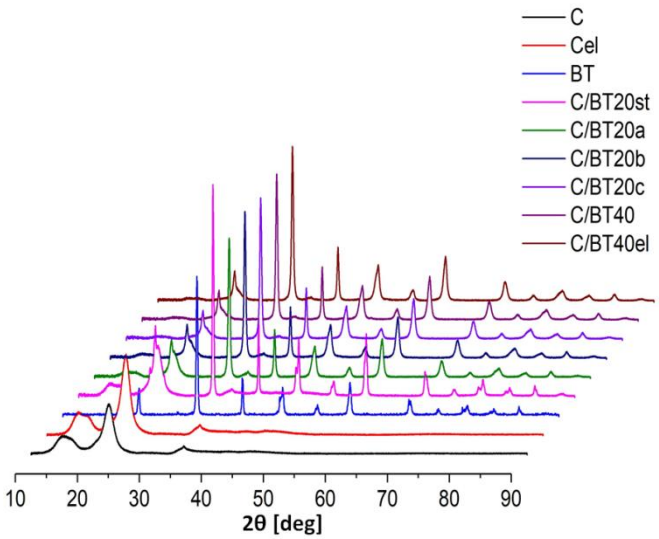

Fig. 3 – WAXD diffractograms of the studied samples.

Microcrystalline cellulose diffractogram presents typical cellulosic pattern for cellulose I with five crystalline peaks at about 15.2º, 16.1º, 20.7º, 22.5º and 34.6º corresponding to (1–10), (110), (102) (200) and (004) crystalline planes and at 18.7º corresponding to amorphous background.[31-35] A similar pattern was observed also for C_{el} diffractogram. BT diffractogram shows specific signals at 22.3º, 31.6º, 38.9º, 45.1 and 45.5º, 50.7 and 51.1º, 56.3º, 65.8º, 70.5º, 74.6 and 75.2º, 79.5º and 83.5º assigned to (100), (110), (111), (002 and 200), (201 and 210), (211), (202), (212), (310), (311) and (222) crystallographic planes of the tetragonal crystalline structure.[36,37]

The analysis of the numerical data in the region $2\theta = 25^{\circ} \div 90^{\circ}$ showed that the diffractograms are identical in terms of BT peak position, the interplanar distances and the relative intensities. For C_{el} and C/BT_{20st} composites no changes were observed when the corresponding diffractograms were was compared to those of cellulose and BT samples. However, one may see that for the other composites obtained under ultrasonic treatment (C/BT_{20a}, C/BT_{20b}, C/BT_{20c}, C/BT_{40}, C/BT_{40el}), the splitting of BT peaks at 2θ = 45.1°-45.5°, 50.7°-- 51.1° and 79.5°-83.5°, which are characteristic to tetragonal phase,[38] seems to disappear. To verify this aspect, the deconvolution of the $2\theta = 44°\div46°$ region was performed for BT and C/BT_{20st}, C/BT_{20c}, C/BT_{40}, C/BT_{40el} composites (Fig. 4). C/BT_{20a} and C/BT_{20b} samples have diffractograms similar to that of C/BT_{20c} (not shown). Indeed, as one may see in Fig 4, the aspect of this the BT peak (splitted into two peaks) is dependent on the preparation conditions and the composite composition. Thus, the sample prepared by stirring, C/BT_{20st}, shows identical peak splitting to pure BT, while ultrasonic irradiation and the thermal treatment under electric field is changing its shape toward a single peak (less evident for the composite containing higher amouns of inorganic particle, C/BT_{40}, not treated under electric field) specific to a cubic phase. Tetragonal-cubic phase rapid transition with increasing temperature and the disappearance of the tetragonal phase at Curie temperature (~120°C for BT) was also observed by Isohama *et al.*[38]

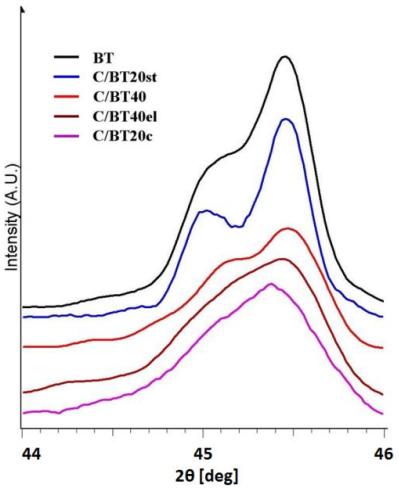

Fig. 4 - WAXD diffractograms of C/BT samples in $2\theta = 44°\div46°$ interval.

The average size of BT crystallites (26.6 nm in pure BT) were only slightly decreased following the introduction into C/BT composites (26.6 nm for

C/BTst; 25.6–26.5 nm for all composites prepared by ultrasonic treatment and heating/ cooling under electric field) as calculated for the (110) plane.

The degree of crystallinity of cellulose in pure cellulose samples and in C/BT composites were determined and are given in Table 3.

Table 3

Degree of crystallinity (χ %) of the studied samples

Sample	C	C_{el}	C/BT_{20st}	C/BT_{20a}	C/BT_{20b}	C/BT_{20c}	C/BT_{40}	C/BT_{40el}
(χ %)	58.2	65.3	62.9	61.5	57.6	51.3	55.6	55.4

As one may observe from Table 3, the degree of crystallinity of pure cellulose increased after the heat treatment in an intense electric field, from 58.2 to 65.3%, while mixing process by mechanical stirring changes very little the crystallinity of cellulose. The homogenization of the composites by ultrasonic irradiation induces noticeable modifications of the crystallinity degree from 61.5% to 51.3% for the composites with 20% BT and to around 55% for the composites with 40% BT. The decrease of the cellulose matrix crystallinity depend on the amplitude of the sonic waves, the ultrasonication time or on the amount of inorganic particles, confirming the structural modifications observed by FT-IR analysis. Similar results were obtained for magnetic composites, where magnetite nanoparticles were acting as projectiles under sonic treatment and disturbed the crystalline phase of cellulose.[8]

The supramolecular structures of the precursors and the obtained composites were identified by SEM analyses (Fig. 5). For BT powder a relatively uniform structure can be noticed. The medium dimensions of the particles range between 400 and 600 nm and the shape is approximately spherical. The SEM micrograph of the pristine microcrystalline cellulose clearly shows well separated fibrils of about 20–40 μm lengths and diameters of around 15 μm. There is no detectable change in SEM micrograph for the heat treated in electric field cellulose sample (C_{el}) as compared to pristine cellulose. For C/BT_{20st} one may observe a non-uniform dispersion of ferroelectric submicronic particles, while the fibers of cellulose do not suffer fragmentation. In the case of C/BT_{20a} and C/BT_{40} samples obtained in milder ultrasonic conditions (Table 1), the deformation and fragmentation of cellulose microfibers is noticed. The increasing of either the ultrasonication time from 15 to 30 min (C/BT_{20b}) or the intensity of the ultrasonic wave from 50% to 100% amplitude (C/BT_{20c}) as well as further thermal treatment under electric field (C/BT_{40el}) promotes a higher fragmentation of the cellulosic fibers, while a better dispersion of BT particles is achieved.

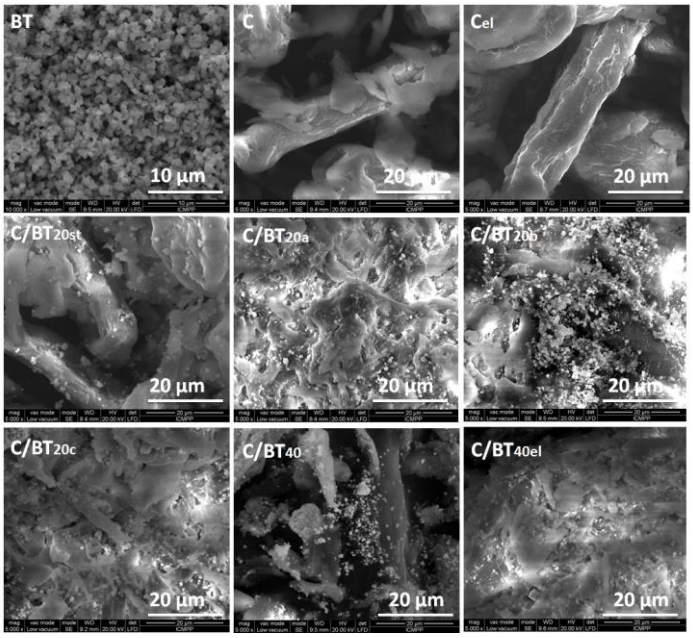

Fig. 5 – SEM micrographs for barium titanate particles (BT), pristine cellulose (C), cellulose thermally treated in electric field (C_{el}) and their composites with BT.

Dielectric properties

The components of the complex dielectric permittivity (dielectric constant, ε', and absorption or loss permittivity, ε'') were measured in the frequency range of 10^{-1}–10^{6} Hz at room temperature. The dielectric constant and dielectric losses of insulating materials are attributed to the polarizations of the electrons and molecules, which includes five types of polarization: electronic, vibrational (or atomic), orientation (or dipolar), ionic and interfacial polarizations. Electronic and vibrational polarizations are ideal for materials used like capacitors because they have small dielectric losses while the ionic and interfacial polarizations result in high dielectric losses and they inherently have long discharge time.[17,39] The variation of these parameters as a function of frequency for barium titanate, cellulose and their composites is depicted in Fig. 6.

In the low frequency domain (up to 10^2 Hz), the dielectric constant (at the same frequency) was found to decrease in the following order: BT >> C/BT_{40el} > C/BT_{40} > C/BT_{20c} > C/BT_{20b} > C/BT_{20a} > C/BT_{20st} > C_{el} > C. One may observe that the presence of 20% ferroelectric precursor (BT) in simply mixed by stirring composite (C/BT_{20st}) induces several times increases of the values of ε′ of composites as compared to that of the pristine cellulose, on the whole range of frequencies (see also Table 4). This was an expected result. For composite samples obtained through ultrasonic treatment, greater values as compared to the mechanically stirred composite were registered, explained by a better homogenization and smaller interfacial polarization. The thermal treatment in electric field also increases ε′ value.

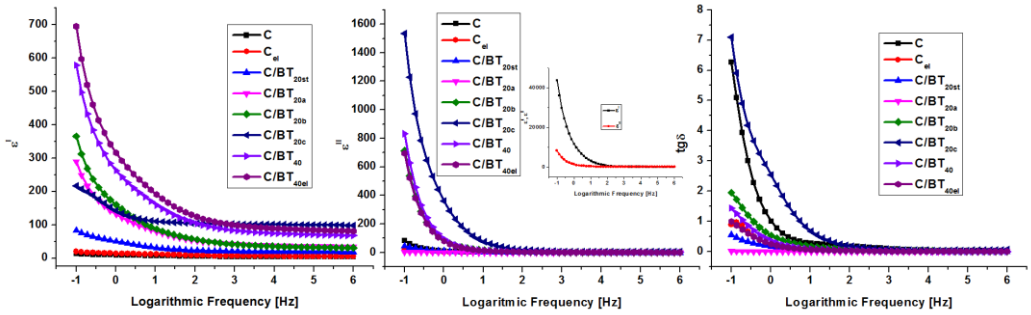

Fig. 6 – Frequency dependency of the real (ε'– dielectric constant) and imaginary part (ε"– loss permittivity) of the complex dielectric constant and frequency dependency of the loss factor (tgδ=ε″/ε′) for the precursors (C, Cel, BT in insert) and their composites.

The dielectric constant, ε' show the energy stored by the capacitor, ε'' show the energy losses (usually in the form of heat, phenomenon that shortens the life of the capacitors). Good capacitors have a loose factor (dissipation factor–tgδ) below 0.3.[17,40,41] For industrial applications in power electronics (power capacitors), the tgδ value for 50–55 Hz (industrial frequency) is important. Table 4 presents the value of ε' and tgδ for the minim and maxim frequency (10^{-1} and 10^{6} Hz), for industrial frequency (50–55 Hz) and for 1000 Hz.

Table 4

ε' and tgδ for precursors and composites at different frequency (ν)

Sample code	ε'				tgδ				E_B [V/ μm]	W [J/cm^3]
ν [Hz]	10^{-1}	50-55	10^3	10^6	10^{-1}	50-55	10^3	10^6		
BT	43665	957	61.3	14.3	0,19	0.09	0.10	0.002	1.4	1.26
C	13.2	6.1	4.6	3.9	6.38	0.21	0.09	0.03	13.1	0.49
C_{el}	19.8	9.2	6.9	5,9	0.90	0.47	0.02	0.007	21.3	1.96
C/BT_{20st}	82.8	24.6	20.0	18,4	0.55	0.07	0.02	0.006	8.9	0.91
C/BT_{20a}	289.4	58.6	40.8	33.7	0.08	$3*10^{-4}$	$1*10^{-4}$	$2*10^{-5}$	17.7	9.01
C/BT_{20b}	365.9	63.4	40.6	30.9	1,95	0.11	0.04	0.008	9.1	2.57
C/BT_{20c}	216.1	105.4	101.6	98.0	7.10	0.27	0.07	0.07	9.9	4.64
C/BT_{40}	578.8	117.1	81.6	67.4	1.44	0.05	0.02	0.04	9.1	4.72
C/BT_{40el}	694.6	140.5	97.9	80.9	1.00	0.04	0.01	0.003	9.7	6.45

As one may see from Table 4, for industrial frequency, the best compromise between ε′ and tgδ values was obtained by C/BT_{20a}. (ε′ = 58.6; tgδ = $=3\cdot10^{-4}$) Composites of dielectric constants higher than 25 at 10^3 were also obtained by using other polymer matrix and different preparation conditions.[42-44]

The dielectric breakdown is known to be controlled by some factors like grain size, homogeneous microstructure (for composites), sample area and thickness, porosity, testing electrode geometry as well as by the strength of bonds (covalent, ionic, Van der Waals).[45,46] The maximum energy storage density, *W* (a parameter of high importance for power capacitors), was calculated with formula 4,[15] by using the measured electrical breakdown strength, E_B (see Experimental part). The values of these E_B and *W* parameters for BT particles (Table 4) are lower, respectively higher than those corresponding to pristine microcrystalline cellulose. The stirred sample (C/BT_{20st}) has the smallest electrical breakdown strength as compared to all other composites. The limited ultrasonication (15 min at 50% amplitude) for C/BT_{20a} sample provides a good homogenization, very good breakdown strength (17.7 kV/mm, surpassed only by C_{el} sample) and the best energy storage density (9.01 J/cm^3) at high voltage. Higher or similar breakdown strength values were obtained by other polymer-based composites, such as low-density polyethylene/clay or fumed silica,[6] poly(vinylidene fluoride-co-chlorotrifluoroethylene)/BT,[44] for polyimide/bypiridine copolymers,[16] or for fully inorganic $Ba_{0.4}Sr_{0.6}TiO_3$/MgO composites,[46] but the storage capacities are much lower. According to the values for dielectric constant, dielectric losses, electrical breakdown strength, and the maximum energy storage density registered in Table 4, C/BT_{20a} sample could be recommended as dielectric material for power capacitors in power electronics industry.

EXPERIMENTAL

Materials

All reagents – microcrystalline cellulose (C), 20 μm, 98%, Aldrich), barium carbonate ($BaCO_3$, 99%, Chemical Company), titanium dioxide (TiO_2, 99%, Chemical Company) – were of analitical grade and used as received. Milli-Q ultrapure distilled water was employed as dispersion medium in ultrasonication experiments.

Preparation of tetragonal barium titanate particles (BT) and of cellulose/barium titanate composites (C/BT)

The following devices were used in the preparation process: Sonics Vibracell ultrasound generator (750W nominal electric power, 20 kHz ultrasound frequencies, provided with sensor for temperature and display for information of the energy delivered to the probe), microwave heating facility (800 W electric power, 2,5 GHz microwave frequency), Specac laboratory press (pressure of 10 tons on a diameter of 13 mm) for preparing samples of cylindrical pellets (diameter, 13 mm; variable thickness as a function of the pressed material amount), and a homemade high voltage (0–30 kV DC) installation.

For BT preparation, the route follows a procedure described in a previous work.[17] Briefly, a 1/2 $TiO_2/BaCO_3$ mixture dispersion in Milli-Q water was ultrasonicated for 60 min. The resulted powder was then separated, dried in a microwave furnace for 10 minutes and thermally treated at 500 °C for 3h to obtain perovskite-like BT submicronic particles (400–600nm).

C/BT composites of different compositions were prepared either by mechanical stirring (st) in Mili-Q water at room temperature at 300 rpm or by ultrasonication in Mili-Q water, followed by drying in an oven (6h at 50 °C). Weight ratios between polymer matrix (C) and ferroelectric microparticles (BT), sonication duration and amplitude were varied. The temperature in the vessel were sonication was made was increasing with time and amplitude of the ultrasonic treatment. Some of the pelleted samples of 13 mm (pristine cellulose-C and C/BT_{40}) were also heated at 80 °C for 15 minutes and left to cool under high electric field induced by an electric potential difference of 30 kV (the distance between electrodes which generate the electric field was 26 mm.

Methods

Infrared spectra of pristine microcrystalline cellulose and its composites with BT were recorded on potassium bromide (KBr) pellets by using a Bruker ALPHA FT-IR spectrometer with 4 cm^{-1} resolution. The concentration of the samples was a constant of 2 mg/200 mg KBr. Processing of the spectra was performed using the Grams 9.1 program (Thermo Fisher Scientific).

The composite surface morphology images were acquired by using an ESEM Quanta 200 Electronic Deflection Microscope.

WAXD analysis was performed on a high resolution Bruker Advance D8 X-ray diffractometer, using Cu-Kα1 radiation, *E* = 8.04 keV, λ = 0.1541 nm, a parallel beam with a Göbel mirror and a dynamic scintillation type detector. The working conditions were as follows: 36 kV, 40 mA, 2s/step, 0.02 degrees/step. All diffractograms were recorded at room temperature (thermostatic at 24°C), in the range 2θ = 10 ÷ 90°. DIFFRAC PLUS Evaluation – XRD Commander, EVA and TOPAS 4-2 softwares were used for data acquisition, for initial and advanced processing, respectively. To be able to compare the results, all samples were made in the same type of support. Thus, the voltages and currents on the tube, the 3 slits, the diffractometric circle distances, the time per step and the angular degree difference were kept identical.

The crystallinity degrees of cellulose (χ) in composites were determined with equation (1), by using Topaz soft mediated extraction of the surface of crystalline BT peak at 22.3, included under the umbrella of the large cellulose peak at 2θ = 20.7–22.5:

$$\chi = A_{cr} \times 100 / A_{tot} \quad (1)$$

where: A_{cr} is the sum of (101), (101), (002) and (012) peak areas and A_{tot} is the total area under diffractogram between 2θ 10–30°, after the extraction of BT peak area.

The average size of BT crystallites of pure $BaTiO_3$ and composite samples was calculated by using Bruker-TOPAZ soft for the (110) plane according to Scherer's equation (2)[46]

$$D = k\lambda/\beta\cos\theta \quad (2)$$

where k = 0.9 – a constant which depends on the shape of the crystallites; λ is the X–ray wavelength (0.1541 nm for Cu catode); β represents the corrected angular width at half maximum intensity in radians, θ is the Bragg angle corresponding to (110) plane.

The dielectric measurements were performed on a Concept 40 Novocontrol Dielectric Spectrometer at room temperature, with silver electrodes, in $10^6 – 10^{-2}$ Hz frequency range on cylindrical pellets (13 mm diameter, 3 mm thickness). The contact surfaces with spectrometer electrodes were covered with silver conductive paste to avoid interfacial polarization and possible edge effects. The dielectric losses were calculated with the relation (3):

$$\mathrm{tg}\delta = \varepsilon'' / \varepsilon' \quad (3)$$

where tgδ represent the dielectric loss; and ε' and ε'' are the real part and the coefficient of the imaginary part of the dielectric permittivity, respectively,

Breakdown strength (E_B) measurements were performed in actuation mode, by applying a ramp signal of 500 V/s on cylindrical pellets of 13 mm diameter, the same density and variable thickness (200–400 μm) placed between two unequal planar circular electrodes arranged coaxially. The high voltage electrode dimensions were 25 mm in radius and 25 mm high. The grounded electrode dimensions were 150 mm in radius and 5 mm high. The voltage was varied in the range 0 ÷ 20 kV (ac) until the breakdown occurred. Five measurements were made for each sample and the average value was taken into account. The maximum energy storage density (W) was calculated by using formula (4).[15]

$$W = E^2_B \cdot (\varepsilon_r \cdot \varepsilon_0)/2 = E^2_B \cdot \varepsilon'/2 \ \ [\mathrm{J/cm^3}] \quad (4)$$

where: ε_r: relative dielectric permittivity, $\varepsilon_0 = 8.854 \cdot 10^{-12}$ F/m: dielectric permittivity for vacuum.

CONCLUSIONS

Cellulose-barium titanate composites were successfully prepared in various compositions through an ultrasound assisted procedure, in the presence or in the absence of a thermal treatment under high electric field. As proved by FT-IR, SEM and WAXD both the structure and the morphology of the studied composite materials are depending on the composition and the preparation conditions. As compared to mechanical stirring, the ultrasonic treatment and the heating/cooling under intense electric filed give rise to more uniformly dispersed BT particles among cellulose microfibers, lower crystallinity degrees of the polymer matrix, reduced size of cellulose fibers when ultrasound intensity or ultrasonic duration are higher. These modifications are the reasons of superior dielectric properties of the composites obtained through ultrasonic treatment. Thus, materials with higher dielectric constants and generally lower (less than 0.3) dielectric losses than the values characteristic to pristine microcrystalline cellulose, for all frequency range between 10^{-1} and 10^6 Hz were obtained. The lower dielectric constants of C/BT composites as compared to those of BT particles are compensated by much higher breakdown strength and energy storage capacity (except the value found for the composite sample prepared by stirring). At industrial frequencies (50–55 Hz), the best compromise in the interplay of the dielectric properties was obtained for C/BT_{20a}, a moderately sonicated sample: ε' = 58.6; tgθ = 0.0003; E_B = 17.7 kV/mm; W = 9.01 J/cm^3.

Acknowledgements. The authors acknowledge the financial support of the Project of the Roumanian Academy entitled "Polymer-inorganic composites and nanostructured materials with applications in photodetection, catalysis and environmental protection".

REFERENCES

1. D. Xu, G. Teng, Y. Heng, Z. Chen, D. Hu, *Mater. Chem. Phys*., **2020**, *249*, 122979.
2. M. Müller, I. Paloumpa, K. Henkel, D. Schmeißer, *Mater. Sci. Eng*., **2006**, *C 26*, 1028-1031.
3. R. Rotaru, C. Peptu, V. Harabagiu, *Cellulose Chem. Techol.*, **2016**, *50*, 621-628.
4. H. Tetsuya, *Bulletin of the Institute for Chemical Research*, Kyoto University, **1962**, *39*, 341-367.
5. B. Schumacher, H. Geßwein, J. Haußelt, T. Hanemann, *Microelectron. Eng.*, **2010**, *87*, 1978-1983.
6. A. T. Mohamed, *Int. J. Electr. Power Energy Syst.*, **2015**, *64*, 469-475.
7. G. Zhang, D. Brannum, D. Dong, L. Tang, E. Allahyarov, S. Tang, K. Kodweis, J. K. Lee, L. Zhu, *Chem. of Mater.*, **2016**, *28*, 4646-660.
8. R. Rotaru, M. Savin, N. Tudorachi, C. Peptu, P. Samoila, L. Sacarescu, V. Harabagiu, *Polym. Chem.*, **2018**, *9*, 860–868.
9. W. Li, J. Yue, S. Liu, *Ultrason. Sonochem.*, **2012**, *19*, 479–485.
10. N. Frone, D. M. Panaitescu, D. Donescu, C. I. Spataru, C. Radovic, R. Trusca, R. Samoghi, *BioResources*, **2011**, *6*, 487–512.
11. Z. Zhao, Z. Mo, C. Feng, J. Wang, *Adv. Mater. Res.*, **2009**, *79-82*, 1543-1546.

12. R. Blinc, "Advanced Ferroelectricity", Chapter 8, in "Electrocaloric effect in ferroelectrics and ferroelectric thin films", University Press Scholarship Online, 2011.
13. U. Kubon, R. Schilling, J. H. Wendorff, *Coll. Polym. Sci.*, **1988**, *266*, 123-131.
14. K. D Schomann, *Appl. Phys.*, **1975**, *6*, 89–92.
15. F. B Madsen, L.Yu, A. E. Daugaard, S. Hvilsted, A. L. Skov, *Polymer*, **2014**, *55*, 6212–6219.
16. X. Peng, W. Xu, L. Chen, Y. Ding, T. Xiong, S. Chen, H. Hou, *React. Funct. Polym.*, **2016**, *106*, 93–98.
17. R. Rotaru, C. Peptu. P. Samoila, V. Harabagiu, *J. Am. Ceram. Soc*., **2017**, *100*, 4511–518.
18. 25. X. Jin, D. Sun, M. Zhang, Y. Zhu, J. Qian, *J. Electroceram*., **2009**, *22*, 285–290.
19. 29. M.A. Ahmed, U. Seddik, N. Okasha, N.G.Imam, *J. Mol. Struct*., **2015**, *1099*, 330–339.
20. M. H Um, C. T Lee, H. Kumasawa, *J. Ind. Eng. Chem*., **1997**, *3*, 251–256.
21. B.D. Stojanovic, A.Z. Simoes, C.O. Paiva-Santos, C. Jovalekic, V.V. Mitic, J.A. Varela, *J. Eur. Ceram. Soc*., **2005**, *25*, 1985–1989.
22. C.-M. Popescu, P.T. Larsson, N. Olaru, C. Vasile, *Polym.*, **2012**, *88*, 530–536.
23. C.-M. Popescu, D. Jones, J. Schalnat, K. Segerholm, M. Henriksson, M. Westin, *Int. J. Biol. Macromol.*, **2020**, *145*, 586–593.
24. E. Robles, N. Izaguirre, B.-I. Dogaru, C.-M. Popescu, I. Barandiaran, J. l Labidi, *Green Chem*., **2020**, 22, 4627.
25. Y. Nishiyama, J. Sugiyama, H. Chanzy, P. Langan, *J. Am. Chem. Soc*., **2003**, *125*, 14300–14306.
26. T. Kondo and S. Dumitriu (Ed.), "Polysaccharides II—Structural Diversity and Functional Versatility", Marcel Dekker, New York, 2005, p. 69–98.
27. S. Perez, K. Mazeau and S. Dumitriu (Ed.), "Polysaccharides II – Structural diversity and functional versatility", Marcel Dekker, New York, 2005, p. 41–68.
28. J. Sugiyama, J. Persson, H. Chanzy, *Macromolecules*, **1991**, *24*, 2461–2466.
29. M. Schwanninger, J. C. Rodrigues, H. Pereira, B. Hinterstoisser, *Vib. Spectros*., **2004**, *36*, 23–40.
30. J. Onyianta, D. O'Rourke, D. Sun, C.-M. Popescu, M. Dorris, *Cellulose*, **2020**, *27*, 7997–8010.
31. C.–M. Popescu, M.–C. Popescu, Gh. Singurel, C. Vasile, D.S. Argyropoulos, S. Willför, *Appl. Spectrosc*., **2007**, *61*, 1168–1177.
32. Z. Cai, J. Kim, *Cellulose*, **2010**, *17*, 83–91.
33. A. F. Tarchoun, D. Trache, T.M. Klapötke, M. Derradji, W. Bessa, *Cellulose*, **2019**, 26, 7635–7651.
34. C.-M. Popescu, P.T. Larsson, N. Olaru, C. Vasile, *Carbohyd. Polym*., **2012**, *88*, 530-536.
35. D. Sun, A. J. Onyianta, D. O'Rourke, G. Perrin, C.-M. Popescu, L. H. Saw, Z. Cai, M. Dorris, *Cellulose*, **2020**, *27*, 3727–3740.
36. H. Y. Choi, Y. G. Jeong, *Composites Part B*, **2019,** *168*, 58–65.
37. M. A. Morsi, M. Abdelaziz, A. H. Oraby, I. Mokhles, *J. Phys. Chem. Solids*, **2019**, *125*, 103–114.
38. Y. Isohama, N. Nakajima, H. Maruyama, Y. Tezuka, T. Iwazumi, *J. Electron Spectroscopy Relat. Phenomena*, **2011**, *184*, 207–209.
39. V. Astapenko, "Polarization Bremsstrahlung on Atoms, Plasmas, Nanostructures and Solids", chapter, "Polarization Bremsstrahlung on Nanostructures", Springer-Verlag Berlin and Heidelberg GmbH & Co. KG, 2013, p. 207–243.
40. P. S. Maruvada and N. Hyltén-Cavallius, *IEEE Transactions on Power Apparatus and Systems*, **PAS-94**, No. 5, September/October 1975, p. 1708–1713.
41. R. Ulrich and L. Schaper, *The International Journal of Microcircuits and Electronic Packaging*, **23**, *2*, Second Quarter**,** 2000, p. 172–180.
42. K. Chiang, R. Popielarz, *Ferroelectrics*, **2002**, *275*, 1–9.
43. Z. H. Dai, J. R. Han, Y. Gao, J. Xu, J. He, B. H. Guo, *Colloid Surface A*, **2017**, *529*, 560–570.
44. Jia, Z. Shao, H. Fan; R. Feng, F. Wang, W. Wang, J. Wang, D. Zhang, Y. Lv, *Compos. Part A*, **2016**, *86*, 1–8.
45. Q. Zhang, L. Wang, J. Luo, Q. Tang, J. Du, *Int. J. Appl. Ceram. Technol.*, **2010**, *7*, 124–128.
46. R. Gerson, T. Marshall, J. Appl.Phys., **1959**, *30*, 1650–1653.
47. A. Patterson, *Phys. Rev.*, **1939**, *56*, 978–982.